Annals of Biomedical Engineering

Integrated stent models based on dimensional reduction. Review and future perspectives

--Manuscript Draft--

Manuscript Number:	
Full Title:	Integrated stent models based on dimensional reduction. Review and future perspectives
Article Type:	S.I. : Stent Bioengineering
Keywords:	Medical stents; mathematical modeling; dimensional model reduction; stent mechanics; drug eluting stents
Corresponding Author:	Paolo Zunino University of Pittsburgh Pittsburgh, UNITED STATES
Corresponding Author Secondary Information:	
Corresponding Author's Institution:	University of Pittsburgh
Corresponding Author's Secondary Institution:	
First Author:	Paolo Zunino
First Author Secondary Information:	
Order of Authors:	Paolo Zunino
	Josip Tambača
	Elena Cutrì
	Suncica Čanić
	Luca Formaggia
	Francesco Migliavacca
Order of Authors Secondary Information:	
Funding Information:	
Abstract:	The characterization of endovascular therapies requires an integrated approach encompassing mechanical analysis of stent expansion and interaction with the artery, the study of the blood flow environment and of fluid dynamics perturbations, and subsequent tissue remodeling possibly modulated by drug release. In this scenario, computational models based on accurate stent geometries represent a widely recognized tool to provide predictive responses. This work reviews the available mathematical and computational approaches that exploit dimensional model reduction to enable a more complete geometrical or physical description of stenting, with an affordable cost on modern computational platforms. Particular attention is devoted to dimensional model reduction of stent mechanics and to model reduction strategies for drug release simulations. Future perspectives on the integration of model reduction approaches for studying biodegradable polymeric stents are eventually discussed.
Suggested Reviewers:	John F LaDisa, Ph.D. Associate Professor of Biomedical Engineering, Director of CV T.E.C. Lab, and Di, Marquette University john.ladisa@marquette.edu
	Alison L Marsden, Ph.D. Associate Professor Jacobs School Faculty Fellow , University of California San Diego amarsden@UCSD.edu

	Alessandro Veneziani, Ph.D. Associate Professor Jacobs School Faculty Fellow , Emory University ale@mathcs.emory.edu
	Maria Paula (Martins Serra) de Oliveira, Ph.D. Full Professor, Universidade de Coimbra poliveir@mat.uc.pt

Integrated stent models based on dimensional reduction.

Review and future perspectives

P. Zunino; J. Tambača; E. Cutrì; S. Čanić; L. Formaggia; F. Migliavacca;

Abstract

The characterization of endovascular therapies requires an integrated approach encompassing mechanical analysis of stent expansion and interaction with the artery, the study of the blood flow environment and of fluid dynamics perturbations, and subsequent tissue remodeling possibly modulated by drug release. In this scenario computational models based on accurate stent geometries represent a widely recognized tool to provide predictive responses.

This work reviews the available mathematical and computational approaches that exploit dimensional model reduction to enable a more complete geometrical or physical description of stenting, with an affordable cost on modern computational platforms. Particular attention is devoted to dimensional model reduction of stent mechanics and to model reduction strategies for drug release simulations. Future perspectives on the integration of model reduction approaches for studying biodegradable polymeric stents are eventually discussed.

Keywords

Medical stents; mathematical modeling; dimensional model reduction; stent mechanics; drug eluting stents;

1. Introduction

Coronary angioplasty with stenting has been accepted as an effective vascular procedure for the treatment of coronary artery disease. Despite its popularity, the success of this approach is still limited due to various clinical complications that may occur after the procedure. Percutaneous coronary interventions have different levels of complexity: from single vessel lesions, bifurcations lesions, to multi-vessel disease, and from focal calcifications to chronic total occlusions. Sub-optimal performance of the stenting procedure has been indicated as a possible cause of complications such as neo-intimal hyperplasia, in-stent restenosis (ISR) and late stent thrombosis. Various studies reported in literature associate these issues to the arterial wall injury (i.e., the rupture of internal elastic lamina) that may occur during the stent deployment (Schwartz, Huber et al. 1992, Rogers, Tseng et al. 1999, Farb, Weber et al. 2002, Gunn, Arnold et al. 2002, Tahir, Hoekstra et al. 2011). A sub optimal stent deployment can also provoke incomplete treatment of the lesion, thrombosis and disturbed flow. Altered local hemodynamics and, in particular, abnormal wall shear stresses (WSS) have been correlated with the onset of ISR (Caro, Fitz-Gerald et al. 1971). In case of drug eluting stents a poor apposition of the stent to the arterial wall reduces drug delivery, which has been associated with impaired arterial wall healing (Cutrì, Zunino et al. 2013, Descovich, Pontrelli et al.). Abnormal hemodynamics due to the presence of stent struts, combined with reduced luminal diameter, may lead to hypoxia (i.e., the deprivation of an adequate oxygen supply) in some regions of the stented coronary artery (Coppola and Caro 2009). Stent fractures, which account for around 29% of all stented lesions with DES (Nakazawa 2009), is a major complication that has been

identified as a possible contributor of adverse events such as ISR (Aoki, Nakazawa et al. 2007),(Lee, Jurewitz et al. 2007), thrombosis (Shite, Matsumoto et al. 2006), myocardial infarction (Makaryus, Lefkowitz et al. 2007), and sudden death (Kang, Kim et al. 2009).

In the last two decades, computational methods have been proposed as a powerful tool in the investigation of the stent performance. The computational approach offers the advantage of allowing the evaluation of fundamental quantities, such as WSS and complex flow conditions, which are hardly detectable by means of in vitro or in vivo experiments (Morlacchi, Keller et al. 2011, Chiastra, Morlacchi et al. 2012).

The most characteristic trait of stents is their complex geometrical pattern. Some examples are shown in Figure 1. The geometrical pattern is determined by many competing criteria such as, for example, longitudinal flexibility, radial stiffness and uniform coverage of the artery for low tissue prolapse and better drug release performance. Because of the complex shapes resulting from the optimization of stent performance, and because of the slender nature of stent struts, the multi-physics simulation of DES using full size stent models is still challenging. Dimensional model reduction consists of the ability to transform computationally heavy 3D models of solid mechanics to model the mechanical properties of stents, into 1D equations accounting for equivalent physical principles but requiring significantly lower computational costs. This modeling approach has shown a remarkable potential for modeling several aspects of vascular stenting (Čanić and Tambača 2012) (D'Angelo, Zunino et al. 2011).

Predicting response of endovascular therapies requires an integrated approach encompassing mechanical analysis of stent expansion and stent interaction with the artery, characterization of the blood flow environment and of fluid dynamics perturbations, and subsequent tissue remodeling. As pointed out in (Kolandaivelu, Leiden et al. 2014) computational and experimental in-vitro or in-vivo models are essential to clarify the intricate interactions between stents and the host artery. The importance of accurate stent geometries for computational models has been synthesized in the recent review (Morlacchi and Migliavacca 2013). There, the construction of the stent geometry has been identified as the initial step in the modeling of mechanical properties of stents, before the constitutive models, realistic loads and boundary conditions are introduced, all of which are essential in simulating the mechanical behavior of stents.

The objective of this contribution is to review the available mathematical and computational approaches that exploit dimensional model reduction to enable a more complete geometrical or physical description of stenting, with an affordable cost on modern computational platforms. Particular attention is devoted to dimensional model reduction of stent mechanics, addressed in Section 2, and to model reduction strategies for drug release simulations, addressed in Section 3. Finally, in Section 4 we discuss the feasibility of integrating model reduction strategies for studying biodegradable polymeric stents, which pose enormous challenges at the level of modeling and simulation. The successful outcome of pursuing this vision will provide unprecedented capabilities of handling complex stent configurations combined with multi-physics description of the device, including mechanics, drug release and biodegradation.

2. Dimensional model reduction for stent mechanics

Modeling stents using 3D approaches requires very fine computational meshes or higher degree polynomials to achieve reasonable accuracy, which implies, among other things, large memory requirements, and high computational costs. Furthermore, to study the performance of stents inserted in native arteries one needs to solve a multi-physics fluid-structure interaction problem in which 3D stent simulations are coupled with the elastodynamics of the native artery, and with 3D blood flow simulations, giving rise to the computational costs that are beyond the computational capabilities of widely available computational platforms.

To get around this difficulty, it was proposed in (Tambača, Kosor et al. 2010) to use dimension reduction, and model the slender stent struts as 1D curved rods. Instead of using 3D elasticity, each stent strut is modeled as a 1D curved rod, which describes the local mechanical properties of each stent strut. The global mechanical properties of an entire stent are then obtained by employing the following three steps:

1. a stent geometry and topology is generated (using ideas from graph theory) giving rise to a 1D stent structure frame in 3D, which we call a **stent net**. Figure 1 shows examples of four different stent net patterns;
2. a mechanical model (i.e., a constitutive relation) for each stent strut is chosen based on the material properties used to manufacture the stent, and a **1D curved rod model** is employed to approximate the mechanical properties of struts;
3. **contact conditions** between stent struts are determined based on the physics of the problem.

Using this approach, the global mechanical properties of stents, such as, e.g., the overall stiffness or the overall bending rigidity, are obtained by solving the mechanical stent net problem described in what follows. The emergent, global mechanical properties of stents follow from the local mechanical properties of each stent strut, and from the way stent struts are arranged in the global stent net geometry.

To describe the methodology used in this dimensional reduction approach we begin by first introducing the 1D curved rod model, then the stent net geometry and the contact conditions.

2.1 1D curved rod model

A curved rod model is a one-dimensional approximation of a slender three-dimensional curved rod-like elastic structure, which is capable of resisting bending and torsion (Figure 2).

A 1D curved rod model is built around a parameterization of the centerline of the rod, given in terms of the arc-length, *s*. At every point s (and time *t* for a dynamic model), the 1D curved rod model captures the displacement *y* of the rod centerline, the rotation θ of the cross-section of the rod, the contact moment *m*, and the contact force *n* at every point *s* (and time *t* for a dynamic model). As an example, we provide here a linearly elastic, 1D curved rod model, which describes well the mechanical properties of stent struts of the fully expanded stents inserted in a native artery. This model captures the relatively small deformation of fully expanded stents under the loading exerted by blood flow and the native artery tissue. The model is given by the following: for a given line force density *f*, find (y,θ,m,n) such that the following balance of contact force and contact moment hold:

$$\begin{aligned} \partial_s n + f &= 0, \\ \partial_s m + t \times n &= 0, \end{aligned} \tag{1}$$

together with the following constitutive relations:

$$\begin{aligned} \partial_s \theta - Q H^{-1} Q^T m &= 0, \\ \partial_s y + t \times \theta &= 0, \end{aligned} \quad \text{with} \quad H = \begin{bmatrix} \mu K & 0 & 0 \\ 0 & EI_b & 0 \\ 0 & 0 & EI_n \end{bmatrix}, \quad \text{where} \quad E = \mu \frac{3\lambda + 2\mu}{\lambda + \mu}, \tag{2}$$

where throughout the entire work ∂_v denotes the partial derivative with respect to the variable v. Here, t is the tangent vector to the middle line, and *Q=(t,n,b)* is the orthogonal matrix containing the tangent vector *t*, the normal *n*, and the bi-normal vector *b* to the middle line, see Figure 2. The vectors *n* and *b* span the normal (orthogonal) plane to the middle line. The Lamé constants are denoted by μ and λ, μK is the torsion rigidity, and I_b and I_n are moments of inertia of the cross-sections. Thus, tensor *H* describes the elastic properties of the curved rod and properties of the cross section. The second equation in (2) states that the centerline of the rod is approximately inextensible, and that the admissible deformations of the cross-section are approximately orthogonal to it. For more details see (Tambača, Kosor et al. 2010).

This model is a linearization of the Antman-Cosserat model for inextensible, unshearable rods, see (Antman 2005) for the nonlinear model (Jurak 2001) and (Canic 2012) for the linearization. It was rigorously shown in (Jurak 2001) that the solution of the 1D model can be obtained as a limit of solutions of equations of 3D linearized elasticity when the thickness of the cross-sections tends to zero. Therefore, for 3D rods that are slender enough, which is the case with stent struts, the 1D curved rod model above provides a consistent approximation of 3D elasticity. Moreover, in (Tambača 2003) it was shown that curved geometry of stent struts can be well approximated with a collection of straight rods, which further simplifies the equations of the 1D model.

2.2. Stent net geometry and coupling of stent struts

The stent net geometry and topology are defined by simply specifying:

1. the set $\mathscr{V}$ of all vertices of the stent net, i.e., the set of all points at which the middle lines of curved rods meet (e.g., the points where stent struts meet), and
2. the set $\mathscr{N}$ of all edges of the stent net, i.e., the set of all middle lines of curved rods connecting different vertices (e.g., the set of all stent struts).

Notice that $(\mathscr{V},\mathscr{N})$ defines a graph, and thus sets the topology of the stent net. By providing the information about the precise geometry of each stent strut via the parameterization of the middle line of each curved rod. Thus, the 1D curved rod model of a 3D stent formed by a family of equations of the form (1), (2), defined on each stent strut (on each edge e_i in $\mathscr{N}$):

$$\begin{aligned} &\partial_s n^i + f^i = 0, \\ &\partial_s m^i + t^i \times n^i = 0, \\ &\partial_s \theta^i - Q^i {H^i}^{-1} {Q^i}^T m = 0, \\ &\partial_s y^i + t^i \times \theta^i = 0. \end{aligned} \tag{3}$$

To complete the definition of the entire stent net problem we need to specify the contact conditions, which hold at the stent net's vertices where stent struts meet. It has been shown that the following two contact (or coupling) conditions are consistent with 3D elasticity (Tambaĉa and Velĉić 2012):

C1. the kinematic coupling condition describing continuity of y and θ of the cross-section, i.e., $y^i=y^j$, $\theta^i=\theta^j$ at v for all the edges i,j meeting at the same vertex v, and

C2. the dynamic coupling condition describing the balance of contact force *n* and contact moment *m* at each vertex of the net, i.e., $\sum_i n^i = 0,\ \sum_i m^i = 0$ where the sum runs over all the edges meeting at a given vertex.

The reduced 1D stent net ($\mathscr{V}$, $\mathscr{N}$) in 3D is now defined as a union of all stent struts modeled as 1D curved rods using equations (3) which hold on every edge in $\mathscr{N}$, satisfying contact conditions C1 and C2 above, which hold at each vertex in $\mathscr{V}$.

2.3. Finite Element Modeling of Stents using the Reduced 1D Stent Net Model

To develop a finite element code for solving the 1D reduced stent net problem it is necessary to write the problem discussed above in the so called weak, or variational formulation. With this formulation it will be apparent that the contact conditions introduced above are natural for this class of problems. The weak formulation for each stent strut is obtained multiplying equations (3) by suitable test functions and integrating the equations by parts. Since stent is defined as a *union* of stent struts, the resulting equations, which hold on each stent strut, are then *added* together to obtain the weak formulation for the entire stent net.

Before this procedure is performed, it is important to discuss how the coupling conditions C1 and C2 above are satisfied. It is natural to require that the kinematic coupling condition C1 is satisfied in the so called *strong sense*, by including this condition into the space of all test functions, thereby requiring that all possible *candidates* for a solution must satisfy the continuity of displacement and the continuity of infinitesimal rotation at every net vertex. The dynamic coupling condition C2, however, is satisfied in the *weak sense* by imposing this condition during integration by parts in the integral formulation of the underlying equations. Since the sum of total

moments and of total forces is zero at each vertex, these terms will cancel out and the resulting weak formulation has a particularly simple form, given below in (4).

More precisely, for the readers who are interested in details, we introduce the space of all *test functions* V_S to consist of all the function $\hat{U} = \left((\hat{y}^1, \hat{\theta}^1) \cdots (\hat{y}^{n_E}, \hat{\theta}^{n_E})\right)$, that are regular enough and satisfy the inextensibility and un-shearability condition $\partial_s \hat{y}^i + t^i \times \hat{\theta}^i = 0$ on each stent strut, and such that the kinematic coupling condition C1 holds at each vertex. Here n_E denotes the total number of edges, i.e., stent struts. We look for solutions $U = \left((y^1, \theta^1) \cdots (y^{n_E}, \theta^{n_E})\right)$ that belong to this test space V_s, such that they satisfy the following weak formulation of the stent net problem:

$$\sum_i^{n_E} \int_{I=1}^{l_i} Q^i H^i Q^{i^T} \partial_s \theta^i \cdot \partial_s \hat{\theta}^i ds = \int_{I=1}^{l_i} f^i \cdot \hat{y}^i ds \qquad (4)$$

for all test functions $\hat{U} = \left((\hat{y}^1, \hat{\theta}^1) \cdots (\hat{y}^{n_E}, \hat{\theta}^{n_E})\right)$, in V_s. This weak formulation holds true not only for the stent problem, but also for any net-like elastic structure problem consisting of slender rods. In (Jurak 2001, Tambača 2003, Griso 2008) it was shown using a rigorous analysis that this model can be obtained from 3D elasticity by letting the thickness of 3D rods be small, as is the case with stent struts.

2.4. Comparison Between the 1D Stent Net Problem and a full 3D Problem

This weak formulation can be easily implemented in a Finite Element code, and run on any platform, including standard personal laptop computers. More details about this approach can be found in (Tambača, Kosor et al. 2010), where a 1D FEM solver was implemented in C++ (Tambača, Kosor et al. 2010). Solutions of the 1D stent net problem were compared to 3D solutions, which were obtained by considering the equations of 3D linearized elasticity defined on the entire stent as a one 3D domain. A

3D Finite Element code was developed using the freely available software package (FreeFem++). P2 finite elements were chosen to simulate the 3D stent. No problems due to locking were detected with this approach. Among several examples considered in (Tambača, Kosor et al. 2010), we present here one in which a uniform stent, as shown in Fig. 3, was subject to a uniform pressure load of 0.5 atm. It was argued in (Tambača, Kosor et al. 2010) that this pressure load is physiologically reasonable, and it may represent the average pressure load that coronary stents are subjected to after their insertion into coronary arteries. The results of the 3D simulations were compared with those of the 1D model of a uniform bare metallic consisting of 2 zig-zag rings, as shown in Fig. 3, corresponding to a uniform, bare metallic stent, made of stainless steel (316L), with the strut thickness of 80μm. The Lamé constants for this stent were given by $\lambda = 1.2 \times 10^{11}$ Pa, $\mu = 8 \times 10^{10}$ Pa.

It was shown in (Čanić and Tambača 2012) that these 3D solutions approach the corresponding *reference* 1D stent net solution, as the 3D mesh was getting more and more refined. The reference 1D solution is the solution for which the relative maximal error between successive approximations obtained with 1D mesh refinement, was smaller than 0.5%. The computational mesh associated with this reference 1D solution uses 474 nodes. The computational mesh associated with the corresponding approximate 3D solution uses 211337 nodes (with maximal tetrahedra edge size of 2.69216×10^{-5} m). The difference in the solution between the 1D and 3D simulations is shown in Figure 3. The 1D reference solution (radial displacement) is shown with red dots, and the corresponding 3D solution is shown in blue color. We see that the 1D model discussed in this section provides an excellent approximation of 3D stent

simulations with significantly less computational costs (one thousand times less computational complexity (211337 nodes in the 3D model v.s. 474 nodes in the 1D model)! Therefore, the 1D approach allows simulations of mechanical properties of stents to be performed on commonly available computational platforms, including personal laptop computers, in real time.

2.5. 1D simulation of a Cypher-like Stent

We conclude this section by showing 1D numerical simulations of the response of a non-uniform stent, such as Cypher stent (Cordis Corporation, Miami Lakes, Florida, USA) shown in Fig. 5 (top), to uniform compression and bending. Additional stents simulations, including Xience-like stent based on Xience™ (Abbott Vascular), Express-like stent based on Express™ (Boston Scienfitic), and Palmaz-like stent based on Palmaz™ (Cordis Corporation), can be found in (Tambaca, Canic et al. 2011).

Figure 5 shows a photograph of a Cypher stent (top), and our numerical simulation of the stent exposed to the uniform pressure load of 0.5 atm using the 1D stent net model. Our simulation indicates that sinusoidal stent struts overall deform much more than the zig-zag stent struts of Fig.3.

Figure 6 shows that relatively large streses are experienced by the sinusoidal struts located near the center of the slightly bent stent. Simulations such as those of Figure 5 and 6 may in future be extended and used to study stent fatigue and fracture in presence of physiological arterial loads. As an example among many others, it was noted in (Nakazawa 2009) that stent fracture in DES, including Cypher, has emerged as a complication following DES implantation, and is recognized as one of the main contributors of in-stent restenosis and possible stent thrombosis. Therefore,

developing computational models that combine a study of mechanical properties of DES together with their anti-thrombogenic action is important in predicting the performance of the currently available DES on the market, and in optimal design of DES for future percutaneous interventions.

3. Dimensional model reduction for Drug Eluting Stent (DES)

The scenario of different approaches for modeling DES is still multi-faceted and a general approach capable of addressing all the DES modeling aspects is not yet available. By searching the extensive literature, we identify a collection of seminal models designed to elucidate what are the fundamental physics regulating DES performance, such as blood flow, vascular mechanics and drug release and diffusion. For example, in the case of (Hwang, Wu et al. 2001, Hwang and Edelman 2002) the effect of strut distribution on drug concentration in the arterial walls is analyzed on the transversal section of an artery. Later, (Balakrishnan, Dooley et al. 2007, Balakrishnan, Dooley et al. 2008) analyzed the role of strut size and their possible superposition on local blood flow using computational fluid dynamics simulations on the longitudinal plane of a cylindrical artery. Another example of mathematical modeling based on idealized geometry are the ones developed by Pontrelli and co-workers (Pontrelli and de Monte 2007, Pontrelli and De Monte 2009, Pontrelli and de Monte 2010) for the analysis of drug release and penetration into the layers characterizing the arterial wall. We also mention the modeling approach adopted by Fortin and Delfour (Delfour, Garon et al. 2005, Bourgeois and Delfour 2008, Delfour and Garon 2010) to study the drug concentration profiles for variable longitudinal strut distribution.

Starting from the previous modeling foundations for the qualitative understanding of DES, computational simulations of DES have evolved towards more accurate geometrical descriptions of these devices. This trend moves along with the constant product innovation, which replaced the simple closed cell patterns with more flexible and less invasive open cell designs. Among many examples we mention (Kolachalama, Levine et al. 2009, Kolachalama, Tzafriri et al. 2009), (Murphy, Savage et al. 2003, Hose, Narracott et al. 2004, Savage, O'Donnell et al. 2004, Grogan, Leen et al. 2013), (Kiousis, Gasser et al. 2007), (Li, Robertson et al. 2012), (Migliavacca, Gervaso et al. 2007, Zunino, D'Angelo et al. 2009, D'Angelo, Zunino et al. 2011, Caputo, Chiastra et al. 2013, Morlacchi, Chiastra et al. 2014).

The development of computational simulators capable to handle realistic stent geometries helps their design in multiple ways. On one hand, it allows for a preliminary assessment of new design concepts, before investing significant resources in animal and clinical trials. A recent example that has considerably stimulated computational studies is the dedicated stents for bifurcating vascular districts (Cutrì, Zunino et al. 2013, Morlacchi, Chiastra et al. 2014). On the other hand, the ability of exactly reproducing stent geometry has allowed simulations using geometrical models reconstructed from clinical images. This technological leap has improved the interaction between computational and in-vivo studies, allowing the quantification of in-silico of factors that cannot be directly measured in-vivo yet, such as WSS. By means of this interdisciplinary approach, correlations between perturbed WSS and ISR have been proved (LaDisa Jr, Olson et al. 2005, Morlacchi, Keller et al. 2011, Caputo, Chiastra et al. 2013, Amatruda, Amatruda et al. 2014, Keller, Amatruda et al. 2014) .

Most of the previously mentioned studies involving accurate representations of realistic stents require using high performance computational platforms, for example commercial multi-processor clusters as well as several man-hours to digitalize the stent geometry and build a computational mesh that fits to the stent design. For static mechanical or fluid dynamics analysis separately, the computational approach has become now an off-the-shelf tool. For the simulation of coupled multi-physics problems involving both aspects, such as stent expansion and the subsequent CFD study possibly combined with drug delivery, the modeling complexity and the related computational cost are still seen as limiting factors for embracing the in-silico approach as a standard design tool (see Figure 7). For the particular case of DES, the main difficulties arise from the need to deal with phenomena that take place on multiple scales. We observe that DES are coated with a microfilm containing the drug that will be locally released into the arterial walls for healing purposes. The thickness of this film generally lay within the range of microns. As regards the time scales, we observe that the release of drug generally persists until days or weeks after the stent implantation. In the following sections we discuss the potential of dimensional model reduction techniques to significantly facilitate the computational analysis of multi-physics problems such as the simulation of DES.

3.1 Modeling drug interaction with arterial walls

The interaction between drug and arterial wall has been modeled using reaction-diffusion equations in several studies (Lovich and Edelman 1996, Sakharov, Kalachev et al. 2002, Tzafriri, Groothuis et al. 2012). For a brief introduction to these models, we follow the lines of (D'Angelo, Zunino et al. 2011) and consider a computational domain Ω_a given by a truncated portion of an artery including both the lumen and the arterial

wall, i.e. $\Omega_a = \Omega_w \cup \Omega_l$ where Ω_w represents the arterial wall and Ω_l is the lumen. A sketch of the domains and their boundaries is shown in Figure 9. Let *a(t,x)* be the drug concentration in the artery, which can be split into $a_l(t,x)$ and $a_w(t,x)$ for the lumen and the wall respectively. According to (Lovich and Edelman 1996, Sakharov, Kalachev et al. 2002) the drug released into the arterial wall can assume two different states: a state where the drug is dissolved into the plasma permeating the interstices between cells, and a state where the drug binds to specific sites of the arterial extracellular matrix. Let $b_w(t,x)$ be the density of the free binding sites, with $b_{w,0}(x)=b_w(t=0,x)$ being their initial density, and let $d_w(t,x)$ be the concentration of the drug attached to the extracellular matrix. The drug in the state d_w can no longer diffuse or be transported by plasma. By virtue of the mass conservation principle, we immediately get $d_w(t,x) = b_{w,0}(x) - b_w(t,x)$. The ligand-receptor interaction between the dissolved drug and the free binding sites is described by equation 5,

$$a_w + b_w \xrightarrow{k_{on}} d_{w,} \quad d_w \xrightarrow{k_{off}} a_w + b_w \tag{5}$$

while for the blood stream we do not account for any chemical interaction. As a result, the transport of drug into the artery can be modeled by means of the following equations:

$$\partial_t a - \nabla \cdot (D_a \nabla a) + \mathbf{u} \cdot \nabla a + k_{on} a b + k_{off}(b - b_0) = 0 \qquad \text{in } \Omega_a \times \mathbb{R}^+$$

$$\partial_t b + k_{on} a b + k_{off}(b - b_0) = 0 \qquad \text{in } \Omega_a \times \mathbb{R}^+$$

$$c = a, \qquad D_a \nabla a \cdot \mathbf{n} = D_c \nabla c \cdot \mathbf{n} \qquad \text{on } \Gamma_s \times \mathbb{R}^+ \qquad (6)$$

$$a = 0 \qquad \text{on } \Gamma_{adv} \times \mathbb{R}^+$$

Equation 6 must be complemented with initial and boundary conditions. We set that initially the artery is drug free and that the drug receptors in the arterial wall are entirely free. For the boundary conditions, it is reasonable to prescribe a vanishing drug concentration at the adventitial side of the artery, denoted with Γ_{adv} (see Figure 9 for an illustration). We observe that Equation 6 cannot be solved yet, because the drug release rate, namely $D_c \nabla c \cdot n$ is not known. One possible approach would be to couple Equation 6 with Equation 7 that describes the drug delivery process. This strategy, which requires modeling the coating as a three-dimensional domain, has been adopted in simplified geometrical configurations, see for example (Zunino 2004). However it is not yet viable for realistic stent geometries, because of exceeding computational costs. This issue can be overcome thanks to model reduction techniques, as described below.

3.1 Dimensional model reduction of drug release from thin coatings

Before implantation, crystalline or amorphous solid drug grains are stored into the stent coating. Drug release to the artery requires a phase transition from solid to liquid phase, usually called *dissolution*. These phenomena have been extensively studied in pharmacology, see for example the seminal works by Higuchi (Higuchi 1961, Higuchi 1963). This field has also attracted the attention of applied mathematicians, with the

final purpose to determine simple formulas for the drug release rate, in spite of the complex governing equations (Cohen and Erneux 1998, Frenning 2003, Frenning 2004). This is also the objective that has motivated the following studies (Formaggia, Minisini et al. 2010, Biscari, Minisini et al. 2011, D'Angelo, Zunino et al. 2011) that are briefly summarized below.

We denote with s and c the drug concentration in solid and dissolved phases respectively, relative to the saturation level of drug in water, c_s . Let Ω_c be the spatial domain occupied by the stent coating, which can be seen as a uniform layer of thickness L covering the stent surface. Then the diffusion-dissolution model reads as follows,

$$\begin{aligned} &\partial_t c - \nabla \cdot (D_c \nabla \mathrm{c}) = \mathrm{K}(s^+)^{2/3}(1-\mathrm{c}) && \text{in } \Omega_c \times \mathbb{R}^+ \\ &\partial_t s = -\mathrm{K}(s^+)^{2/3}(1-\mathrm{c}) && \text{in } \Omega_c \times \mathbb{R}^+ \qquad (7) \\ &s = s_{0,} \quad \mathrm{c} = 0 && \text{in } \Omega_c \times \{t = 0\} \end{aligned}$$

where K is the dissolution constant and D_c is the diffusivity of drug within the coating layer, typically modeled as a porous polymeric substrate. The right hand sides of the equations above correspond to the Noyes–Whitney formula, a well-accepted model for the dissolution rate (Macheras and Iliadis 2006). Ever since the development of the early models of controlled drug release it has been well known that the interaction between dissolution (reaction type terms) and diffusion is essential to determine the drug release rate. The parameter $\Lambda = D_c/(K \times L^2)$ regulates the interplay between these two factors.

Since drug diffuses very slowly in the stent coating, it is reasonable to study Equation (7) in the small diffusivity regime, namely for *Λ<<1.* Using asymptotic expansions, an approximate solution of the problem was derived analytically in (Biscari, Minisini et al. 2011) giving rise to a simple expression for the drug release rate $J(t)$ determined by the diffusion-dissolution model:

$$J(t) = -\big(1 - a(t)\big)(\mathrm{erf}(\Gamma))^{-1}\sqrt{\frac{D_c}{\pi t}}, \quad \mathrm{t} \in (0, \mathrm{T} = L^2/(4D_c\Gamma^2)) \tag{8}$$

where Γ is such that $\frac{\exp(-\Gamma^2)}{\sqrt{\pi}\Gamma erf(\Gamma)} = \frac{s_0 - 1}{1 - a}$

a being the drug concentration in the exterior, typically the blood stream or the arterial wall. Therefore, the formula above can be utilized as a boundary condition for the model that regulates the interaction of the drug with blood stream and arterial walls. This approach has the advantage of enabling the study of drug release in the artery without requiring the cumbersome solution of Equation 7.

The computational model that combines Equation 6 and 8 was used in (Migliavacca, Gervaso et al. 2007, Vergara and Zunino 2008, Zunino, D'Angelo et al. 2009) with increasing levels of complexity for the constitutive laws characterizing drug release and drug-artery interactions. Thanks to the reduced computational costs of solving models such as the one in Equation 8, a full simulation of stent expansion, blood flow analysis and drug release was performed for the first time on a realistic design of a single stent cell in (Zunino, D'Angelo et al. 2009). The simulation of a full stent model was still too challenging at the time. This limitation motivated the development of new model reduction techniques to improve the performance of DES simulation, which is reviewed in the next section.

3.2 Dimensional reduction of stent struts for modeling drug release

As pointed out in the introduction, the most characteristic trait of stents is their complex geometrical pattern. Because of the complex shapes, the multi-physics simulation of DES using realistic and full size stent models is still challenging. The model reduction technique proposed in Section 3.1 facilitates the simulation of DES but is not sufficient to enable simulation of DES using realistic geometries. Following the approach by D'Angelo for modeling capillaries and small vessels embedded into biological tissues (D'Angelo and Quarteroni 2008, D'Angelo 2010), the sequence of works (D'Angelo and Zunino 2009, D'Angelo, Zunino et al. 2011, Cutrì, Zunino et al. 2013, Morlacchi, Chiastra et al. 2014) explores how to simplify the cumbersome issue of using a real stent design for simulations of drug release without excessive computational costs. Coherently with the models discussed in Section 2, stents can be described as one-dimensional networks of curved rods (called struts). With respect to DES, each strut interacts with the artery by releasing an amount of drug that depends on the release rate, determined by Equation 8, and by the extension of the coated surface. The idea proposed in (D'Angelo and Quarteroni 2008) enables to model drug release using concentrated sources of drug distributed along one-dimensional curves that follow the stent pattern. This approach, depicted graphically in Figure 9, consists to replace Equation (6) with the following one

$$\begin{aligned} &\partial_t a - \nabla \cdot (D_a \nabla a) + \mathbf{u} \cdot \nabla a = F_a \delta_\Lambda + \partial_t b && \text{in } \Omega_a \times \mathbb{R}^+ \\ &\partial_t b + k_{on} a b + k_{off}(b - b_0) = 0 && \text{in } \Omega_a \times \mathbb{R}^+ \end{aligned} \tag{9}$$

where the right hand side $F_a \delta_\Lambda$ models struts as concentrated sources for drug release. In particular, δ_Λ denotes a distribution of Dirac masses along the strut longitudinal

midline Λ_s . For simplicity, the stent cross-section is assumed to be constant and it is quantified by the equivalent radius R (see also Figure 9) Finally F_a is a release rate calculated using Equation (8) that defines the mass flux per unit area over the strut surface Γ_s. As a result, at any specific point *s* along the stent midline we have,

$$F_a(t,s;a) = \frac{2\pi \mathrm{R}}{\mathrm{erf}(\Gamma)}\sqrt{\frac{D_c}{\pi t}}\big(1-\bar{a}(s)\big)\xi(s)$$

$$\bar{a}(s) = \frac{1}{|\gamma(s)|}\int_{\gamma(s)} a(s,\theta,R)\,d\,\theta \qquad (10)$$

We notice that Equation (9) and (10) account for the actual stent graph (Λ) and the strut thickness (*R*).

The approach that uses 1D-struts (Figure 9) features significant advantages with respect to the one based on 3D stent geometry (Figure 8). For example, in the former case, the finite element discretization of Equation (9) does not require that the computational mesh of the artery conform to the one of the stent. In other words, th6 computational mesh of artery and stent are completely independent. This increased flexibility made possible the study (Cutrì, Zunino et al. 2013) where simulations of drug distribution in arterial bifurcations treated with multiple stents was performed. In particular, the effect of different stenting protocols, such as Provisional Side Branch (PSB), Culotte, (CU), inverted Culotte (ICU), and the implantation of a newly designed dedicated stent for bifurcations (TRY) was analyzed. These complex stent configurations are visualized in Figure 10. Thanks to the ability of easily perturbing the stent configuration without changing other parts of the geometrical model, the effect of malapposition on drug release was also quantified.

One limitation of using one-dimensional approximation of stent struts is that the stent is transparent to flow, which means that flow perturbation due stent struts exposed to blood stream cannot be studied without additional modeling efforts. An extension of the current model to account for flow perturbations would be beneficial and it is in order.

4 Towards the integration of dimensionally reduced models for biodegradable polymeric stents

Biodegradable polymeric materials are ubiquitous in medicine. We mention biodegradable sutures, pins and screws for orthopedic surgery and tissue engineering scaffolds, among many other remarkable examples. The trend of replacing permanent materials with degradable ones has recently expanded to the development of medical stents, see (Colombo and Karvouni 2000, Moore Jr, Soares et al. 2010). Advantages of biodegradable implants include: (i) decreased risk of late stent thrombosis (ii) prolonged antiplatelet therapy may not be strictly necessary; (iii) a polymeric stent is a reservoir for the incorporation of drugs and polymer degradation and erosion may enhance drug release kinetics; (iv) biodegradable stents are compatible with MRI and MSCT imaging.

The pioneering employment of biodegradable polymers as design material in a cardiovascular stent dates back to the late 1980s at Duke University by Stack and co-workers. A specialized form of polylactic acid was chosen among several absorbable polymers to construct an open mesh, self-expanding stent. In another attempt to establish the feasibility of biodegradable stents, a balloon-expandable biodegradable stent made of polyglycolic acid was deployed in coronary arteries of dogs at Kyoto University. In (Tamai, Igaki et al. 1999, Tamai, Igaki et al. 2000, Tsuji, Tamai et al.

2000) the first report on the immediate and 6-month results after implantation of their biodegradable poly-L-lactic acid stents in humans is provided.

The desing of biodegradable stents is a challenging problem because it involves the coupling of biomechanics and polymer biochemistry, in order ot utlimately determine the degradation rate in vivo. Their study involves complex equations that depend on a high dimensional parameter space. In this context, mathematical and computational modeling in general, and reduced models in particular, turn out to be valuable tools to provide insight on the problem and to guide experiments. In the case of biodegradable metal stents, not addressed here, we mention the extensive work by Wu et al. (Wu, Petrini et al. 2010, Wu, Gastaldi et al. 2011, Wu, Chen et al. 2013, Demir, Previtali et al. 2014, Petrini, Wu et al. 2014).

Many factors influence biodegradation, such as temperature, enzymes, radiation, hydrolysis and machanical loading. For biodegradable stents in vivo, mechanical loads and hydrolisis play a significant role (Weir, Buchanan et al. 2004, Moore Jr, Soares et al. 2010, Soares, Moore et al. 2010). In particular, it is observed that at locations where strain is the highest, material deteriorates more rapidly. In this section we discuss how the dimensionally reduced models proposed for stent mechanics and drug release can be naturally combined in order to describe the degradation process.

A model for degradation under mechanical loading was derived in (Rajagopal, Srinivasa et al. 2007) and used by Soares in (Soares, Moore et al. 2008). This model is based on the concept of degradation function, denoted by d.It is initialy set to 1 and it decreases in time until the value of $d=0$ is reached, which corresponds to a fully degraded unable

to bear loads. The spatio-temporal evolution of the degradation process is described by the following equation,

$$\partial_t d - a\partial_{ss} d = \sigma \tag{11}$$

where α is a diffusion coefficient (α=0 is possible) and σ is a given function that represents the degradation rate and quantifies how it depends on mechanical stresses, hydrolysis and other factors that affect polymer chains cleavage. Here, we envision a model where a biodegradable polymer is described as a mixture of different molecules, called oligomers, whose molecular weight constantly change under the factors that promote polymer degradation. Cleavage of large oligomers into smaller ones determines material degradation, while loss of small polymer chains from the stent is called material erosion. Both effects may happen simultaneously. As a result, we postulate the following functional form of the degradation function,

$$\sigma = \sigma(d(s,t), \partial_s[y,\theta](s,t), [\rho,x](s,t)) \tag{12}$$

where $[y,\theta]$ denote the dependence of degradation from the deformation state of the material, while $[\rho,x]$ are the polymer average density and degree of polymerization and account for the role of hydrolysis on the degradation process. In the following section we discuss how equations (11) and (12) can be cambined with the previously described reduced models for stent mechanics and mass transfer.

4.1 Modeling polymer degradation and erosion by hydrolisis

Hydrolysis is the main cause of degradation for synthetic aliphatic polyesters such as polylactic acid (PLA) (Weir, Buchanan et al. 2004), commonly used for biodegradable stents. To describe degradation and erosion of polymer matrices we follow the approach of (Gopferich 1997, Göpferich 1997, Siepmann and Göpferich 2001,

Burkersroda, Schedl et al. 2002) and in particular the general formulation proposed in (Soares and Zunino 2010) . Polymers such as PLA are described as a poly-disperse mixture of monomer chains whose bonds can be cleaved by interaction with water. Molecular diffusion and water absorption are also allowed. In case the polymer matrix is loaded with a drug, the model can be easily adapted to account for drug release. The resulting model can be summarized in the following equations for diffusion and cleavage of polymer chains of length (*i*), water absorption and drug release respectively:

$$\begin{aligned} &\partial_t \rho_i = \nabla \cdot (D_i \nabla \rho_i) + \sum_{j=1}^{N} A_{ij} \rho_j, \quad for\ i = 1, \dots, N, \\ &\partial_t \rho_w = \nabla \cdot (D_w \nabla \rho_w) - f_w, \\ &\partial_t \rho_d = \nabla \cdot (D_d \nabla \rho_d) \end{aligned} \tag{13}$$

where ρ_i, ρ_w, ρ_d are polymer, water and drug partial densities and D_i, D_w, D_d are the polymer, water and drug diffusivities. Hydrolysis is described by the coefficients $A_{ij}(\rho_w)$, which quantify the rate at which large chains transform into smaller ones, because of hydrolysis, as a function of water mass fraction within the mixture. Simultaneously, $f_w(\rho_i)$ models how much water is consumed by the same reactions. We refer to (Soares and Zunino 2010) for further details about the mathematical model. As shown there, the solution of these equations by means of numerical techniques determine how the average degree of polymerization (x) and the average polymer density (ρ), evolve in time and across the stent strut thickness (denoted with the variable z in the following plots). An outline of the results is reported in Figure 11. These results provide significant insight on modeling biodegradable stents. Figure 11 (a) confirms that hydrolysis has an important role on degradation. Indeed, it shows that because of interaction with water,

PLA chains quickly degrade to a mixture of smaller molecules. This effect likely entails a non-negligible transformation of the material properties. As a result, we conclude that it is essential to account for the role of the average degree of polymerization in the degradation function introduced before. Results (b) and (c) illustrate the process of mass loss, or material erosion. They confirm that the model can capture bulk and surface erosion behaviors. Figure 11 (b) shows bulk erosion, a uniform loss of material from a polymer slab, which happens when diffusion phenomena dominate over hydrolysis. Surface erosion occurs in the opposite case, namely when hydrolysis takes place with a faster peace than diffusion phenomena. If this would be the case for biodegradable stents, the strut section would remain intact but it would progressively shrink. Once two characteristic behaviors have been identified, model reduction techniques can come into play in order to mitigate the complexity of the polymer degradation model in each of those distinct regimes. For example, the asymptotic expansion techniques addressed in section 3.2 can be applied to obtain a simplified expression for the variation of the average polymer density with respect to time. Indeed, we observe that in the small diffusion regime, Equations 7 and Equation 13 share a very similar nature, leading to similar solutions called traveling waves and actually visualized in Figure 11 (c). The corresponding surrogate models will be then easily plugged into the expression for the degradation rate (σ), and ultimately into a model for the mechanics of a biodegradable stent, as described in the next section.

4.2 Dimensionally reduced mechanical modesls for biodegradable stents

In (Tambača and Žugec 2015) the ideas from (Jurak 2001, Soares, Moore et al. 2008, Tambača, Kosor et al. 2010) were used to derive a quasistatic 1D model of

biodegradable curved rods. The resulting model is nonlinear, and is given in terms of displacement and degradation as two unknown functions. The model can be viewed as a system of 1D curved rods, similar to (1) and (2) with degradation □ appearing as a coefficient, plus an additional equation modeling the evolution of degradation using the solution of the 1D curved rod model. More precisely, the 1D model of biodegradable curved rods from (Tambača and Žugec 2015) is given by:

$$\begin{aligned} &\partial_s n + df + h = 0 \\ &\partial_s m + t \times n = 0 \\ &d\partial_s \theta - QH^{-1}Q^T m = 0 \\ &\partial_s y + t \times \theta = 0 \end{aligned} \tag{14}$$

This 1D model is obtained from the three-dimensional equations of biodegradable elastic rod-like bodies, see (Soares, Moore et al. 2008, Soares, Moore et al. 2010), using formal asymptotic expansion with respect to the small thickness of the rod. Even though the system is nonlinear one can show that system (14) has at least one solution for some finite time, and that with the initial condition $d = 1$ and appropriate boundary conditions, the solution is also unique. Additionally to the assumptions from (Soares, Moore et al. 2008) it was also assumed that: 1) the stress and strain in the body are small so linearized elasticity (with coefficients depending on degradation) is well suited in the model; 2) a small diffusion effect is present in the three-dimensional model, see (Soares, Moore et al. 2010, Soares and Zunino 2010); and 3) degradation is much faster than the oscillations of the elastic body. As a consequence the behavior is quasistatic in the sense that the inertial term in the evolution equation for the elastic body can be neglected. This explains the form of the equations in (14).

In Figure 12 we present a numerical simulation of the 1D model (4) for a simplified form of the degradation function, which only depends on the mechanical deformations, namely we use $\sigma = \sigma(d \cdot \partial_s \theta)$ for a single rod clamped at both ends, exposed to a constant contact force. Five different colors denote five time snap-shots from t = 0 to t = 400 (time steps). Simulations show that this simple model qualitatively captures the expected effects of degradation on stent mechanics. One can see that as the material degrades the displacement grows in time, as shown on the left panel and at each point along the rod degradation rate linearly decreases with time. As a consequence, the material degrades completely in finite time (which depends on the parameters in the problem). The rate of degradation is approximately uniform along the stent.

5 Conclusions

There is consensus on the importance of modeling (in-silico, in-vitro or in-vivo) to improve the predictions on the outcome of endovascular therapies (Kolandaivelu, Leiden et al. 2014) . Computational models also play a role in the design phase of the device, in particular for the new generation of biodegradable stents. However, as it is observed in (Morlacchi and Migliavacca 2013), when modeling is needed most, such as for stenting bifurcations for example, computational cost and considerable efforts required to implement the model into a general purpose commercial platform, often limit the potential of computational approaches. Model reduction techniques represent a valuable, but still rather unexplored tool to overcome these limitations. The essence of model reduction is to synthesize into surrogate equations the most significant traits of the problem, in this case modeling vascular stents. Although considerable resources must be dedicated to the development of prototype simulators, these new approaches

enable to push forward the frontier of stent modeling beyond the current limits. Thanks to the dimensional model reduction applied to stent mechanics and drug release, challenging tasks such as simulating stent fatigue tests or studying drug release patterns into an arterial bifurcation can be achieved on standard (single processor) computational platforms within reasonable time. We hope that this review will help spreading the use of this modeling approach within the community active in developing medical stents technology.

References

Amatruda, C. M., C. M. Amatruda, C. B. Casas, B. K. Keller, H. Tahir, G. Dubini, A. Hoekstra, A. Hoekstra, D. Rodney Hose, D. Rodney Hose, P. Lawford, P. Lawford, F. Migliavacca, A. Narracott, A. Narracott, J. Gunn and J. Gunn (2014). "From histology and imaging data to models for in-stent restenosis." International Journal of Artificial Organs **37**(10): 786-8800.

Antman, S. (2005). Nonlinear Problems of Elasticity, Springer.

Aoki, J., G. Nakazawa, K. Tanabe, A. Hoye, H. Yamamoto, T. Nakayama, Y. Onuma, Y. Higashikuni, S. Otsuki, A. Yagishita, S. Yachi, H. Nakajima and K. Hara (2007). "Incidence and clinical impact of coronary stent fracture after sirolimus-eluting stent implantation." Catheterization and Cardiovascular Interventions **69**(3): 380-386.

Balakrishnan, B., J. Dooley, G. Kopia and E. R. Edelman (2008). "Thrombus causes fluctuations in arterial drug delivery from intravascular stents." Journal of Controlled Release **131**(3): 173-180.

Balakrishnan, B., J. F. Dooley, G. Kopia and E. R. Edelman (2007). "Intravascular drug release kinetics dictate arterial drug deposition, retention, and distribution." Journal of Controlled Release **123**(2): 100-108.

Biscari, P., S. Minisini, D. Pierotti, G. Verzini and P. Zunino (2011). "Controlled release with finite dissolution rate." SIAM Journal on Applied Mathematics **71**(3): 731-752.

Bourgeois, É. and M. C. Delfour (2008). "General patterns and asymptotic dose in the design of coated stents." Computer Methods in Biomechanics and Biomedical Engineering **11**(4): 323-334.

Burkersroda, F. V., L. Schedl and A. Göpferich (2002). "Why degradable polymers undergo surface erosion or bulk erosion." Biomaterials **23**(21): 4221-4231.

Čanić, S. and J. Tambača (2012). "Cardiovascular stents as PDE nets: 1D vs. 3D." IMA Journal of Applied Mathematics (Institute of Mathematics and Its Applications) **77**(6): 748-770.

Canic, S. T., J (2012). "Cardiovascular Stents as PDE Nets: 1D vs. 3D." IMA Journal of Applied Mathematics **77**(6): 748-779.

Caputo, M., C. Chiastra, C. Cianciolo, E. Cutrì, G. Dubini, J. Gunn, B. Keller, F. Migliavacca and P. Zunino (2013). "Simulation of oxygen transfer in stented arteries and correlation with in-stent restenosis." International Journal for Numerical Methods in Biomedical Engineering **29**(12): 1373-1387.

Caro, C. G., J. M. Fitz-Gerald and R. C. Schroter (1971). "Atheroma and arterial wall shear. Observation, correlation and proposal of a shear dependent mass transfer mechanism for atherogenesis." Proceedings of the Royal Society of London. Series B. Biological sciences **177**(46): 109-159.

Chiastra, C., S. Morlacchi, S. Pereira, G. Dubini and F. Migliavacca (2012). "Computational fluid dynamics of stented coronary bifurcations studied with a hybrid discretization method." European Journal of Mechanics, B/Fluids **35**: 76-84.

Cohen, D. S. and T. Erneux (1998). "Controlled drug release asymptotics." SIAM Journal on Applied Mathematics **58**(4): 1193-1204.

Colombo, A. and E. Karvouni (2000). "Biodegradable stents: 'Fulfilling the mission and stepping away'." Circulation **102**(4): 371-373.

Coppola, G. and C. Caro (2009). "Arterial geometry, flow pattern, wall shear and mass transport: Potential physiological significance." Journal of the Royal Society Interface **6**(35): 519-528.

Cutrì, E., P. Zunino, S. Morlacchi, C. Chiastra and F. Migliavacca (2013). "Drug delivery patterns for different stenting techniques in coronary bifurcations: A comparative computational study." Biomechanics and Modeling in Mechanobiology **12**(4): 657-669.

D'Angelo, C. (2010). "Finite element approximation of elliptic problems with dirac measure terms in weighted spaces. Applications to 1D-3D coupled problems." MOX Report 39/2010.

D'Angelo, C. and A. Quarteroni (2008). "On the coupling of 1D and 3D diffusion-reaction equations. Application to tissue perfusion problems." Mathematical Models and Methods in Applied Sciences **18**(8): 1481-1504.

D'Angelo, C. and P. Zunino (2009). "Multiscale models of drug delivery by thin implantable devices." Applied and Industrial Mathematics in Italy III, Ser. Adv. Math. Appl. Sci. **82**: 298-310.

D'Angelo, C., P. Zunino, A. Porpora, S. Morlacchi and F. Migliavacca (2011). "Model reduction strategies enable computational analysis of controlled drug release from cardiovascular stents?" SIAM Journal on Applied Mathematics **71**(6): 2312-2333.

Delfour, M. C. and A. Garon (2010). "New equations for the dose under pulsative/periodic conditions in the design of coated stents." Computer Methods in Biomechanics and Biomedical Engineering **13**(1): 19-34.

Delfour, M. C., A. Garon and V. Longo (2005). "Modeling and design of coated stents to optimize the effect of the dose." SIAM Journal on Applied Mathematics **65**(3): 858-881.

Demir, A. G., B. Previtali, Q. Ge, M. Vedani, W. Wu, F. Migliavacca, L. Petrini, C. A. Biffi and M. Bestetti (2014). "Biodegradable magnesium coronary stents: Material, design and fabrication." International Journal of Computer Integrated Manufacturing **27**(10): 936-945.

Descovich, X., G. Pontrelli, S. Melchionna, S. Succi and S. Wassertheurer (2013). "Modeling fluid flows in distensible tubes for applications in hemodynamics." International Journal of Modern Physics C **24**(5).

Farb, A., D. K. Weber, F. D. Kolodgie, A. P. Burke and R. Virmani (2002). "Morphological predictors of restenosis after coronary stenting in humans." Circulation **105**(25): 2974-2980.

Formaggia, L., S. Minisini and P. Zunino (2010). "Modeling polymeric controlled drug release and transport phenomena in the arterial tissue." Mathematical Models and Methods in Applied Sciences **20**(10): 1759-1786.

Frenning, G. (2003). "Theoretical investigation of drug release from planar matrix systems: Effects of a finite dissolution rate." Journal of Controlled Release **92**(3): 331-339.

Frenning, G. (2004). "Theoretical analysis of the release of slowly dissolving drugs from spherical matrix systems." Journal of Controlled Release **95**(1): 109-117.

Gopferich, A. (1997). "Mechanisms of polymer degradation and elimination." Handbook of Biodegradable Polymers: 451-471.

Göpferich, A. (1997). "Bioerodible implants with programmable drug release." Journal of Controlled Release **44**(2-3): 271-281.

Griso, G. (2008). "ASYMPTOTIC BEHAVIOR OF STRUCTURES MADE OF CURVED RODS." Analysis and Applications **06**(01): 11-22.

Grogan, J. A., S. B. Leen and P. E. McHugh (2013). "Optimizing the design of a bioabsorbable metal stent using computer simulation methods." Biomaterials **34**(33): 8049-8060.

Gunn, J., N. Arnold, K. H. Chan, L. Shepherd, D. C. Cumberland and D. C. Crossman (2002). "Coronary artery stretch versus deep injury in the development of in-stent neointima." Heart **88**(4): 401-405.

Higuchi, T. (1961). "Rate of release of medicaments from ointment bases containing drugs in suspension." Journal of pharmaceutical sciences **50**: 874-875.

Higuchi, T. (1963). "MECHANISM OF SUSTAINED-ACTION MEDICATION. THEORETICAL ANALYSIS OF RATE." Journal of pharmaceutical sciences **52**: 1145-1149.

Hose, D. R., A. J. Narracott, B. Griffiths, S. Mahmood, J. Gunn, D. Sweeney and P. V. Lawford (2004). "A thermal analogy for modelling drug elution from cardiovascular stents." Computer Methods in Biomechanics and Biomedical Engineering **7**(5): 257-264.

Hwang, C. W. and E. R. Edelman (2002). "Arterial ultrastructure influences transport of locally delivered drugs." Circulation Research **90**(7): 826-832.

Hwang, C. W., D. Wu and E. R. Edelman (2001). "Physiological transport forces govern drug distribution for stent-based delivery." Circulation **104**(5): 600-605.

Jurak, M. T., J. (2001). "Linear curved rod model. General curve." Mathematical Models and Methods in Applied Sciences **11**(7): 1237-1252.

Kang, W. Y., W. Kim and S. H. Hwang (2009). "Dark side of drug-eluting stent: Multiple stent fractures and sudden death." International Journal of Cardiology **132**(3): e125-e127.

Keller, B. K., C. M. Amatruda, D. R. Hose, J. Gunn, P. V. Lawford, G. Dubini, F. Migliavacca and A. J. Narracott (2014). "Contribution of Mechanical and Fluid Stresses to the Magnitude of In-stent Restenosis at the Level of Individual Stent Struts." Cardiovascular Engineering and Technology **5**(2): 164-175.

Kiousis, D. E., T. C. Gasser and G. A. Holzapfel (2007). "A numerical model to study the interaction of vascular stents with human atherosclerotic lesions." Annals of Biomedical Engineering **35**(11): 1857-1869.

Kolachalama, V. B., E. G. Levine and E. R. Edelman (2009). "Luminal flow amplifies stent-based drug deposition in arterial bifurcations." PLoS ONE **4**(12).

Kolachalama, V. B., A. R. Tzafriri, D. Y. Arifin and E. R. Edelman (2009). "Luminal flow patterns dictate arterial drug deposition in stent-based delivery." Journal of Controlled Release **133**(1): 24-30.

Kolandaivelu, K., B. B. Leiden and E. R. Edelman (2014). "Predicting response to endovascular therapies: Dissecting the roles of local lesion complexity, systemic comorbidity, and clinical uncertainty." Journal of Biomechanics **47**(4): 908-921.

LaDisa Jr, J. F., L. E. Olson, R. C. Molthen, D. A. Hettrick, P. F. Pratt, M. D. Hardel, J. R. Kersten, D. C. Warltier and P. S. Pagel (2005). "Alterations in wall shear stress predict sites of neointimal hyperplasia after stent implantation in rabbit iliac arteries." American Journal of Physiology - Heart and Circulatory Physiology **288**(5 57-5): H2465-H2475.

Lee, M. S., D. Jurewitz, J. Aragon, J. Forrester, R. R. Makkar and S. Kar (2007). "Stent fracture associated with drug-eluting stents: Clinical characteristics and implications." Catheterization and Cardiovascular Interventions **69**(3): 387-394.

Li, D., A. M. Robertson, G. Lin and M. Lovell (2012). "Finite element modeling of cerebral angioplasty using a structural multi-mechanism anisotropic damage model." International Journal for Numerical Methods in Engineering **92**(5): 457-474.

Lovich, M. A. and E. R. Edelman (1996). "Computational simulations of local vascular heparin deposition and distribution." American Journal of Physiology - Heart and Circulatory Physiology **271**(5 40-5): H2014-H2024.

Macheras, P. and A. Iliadis (2006). "Modeling in biopharmaceutics pharmacokinetics, and pharmacodynamics." Interdiscip. Appl. Math **30**: 30.

Makaryus, A. N., L. Lefkowitz and A. D. K. Lee (2007). "Coronary artery stent fracture." International Journal of Cardiovascular Imaging **23**(3): 305-309.

Migliavacca, F., F. Gervaso, M. Prosi, P. Zunino, S. Minisini, L. Formaggia and G. Dubini (2007). "Expansion and drug elution model of a coronary stent." Computer Methods in Biomechanics and Biomedical Engineering **10**(1): 63-73.

Moore Jr, J. E., J. S. Soares and K. R. Rajagopal (2010). "Biodegradable Stents: Biomechanical Modeling Challenges and Opportunities." Cardiovascular Engineering and Technology **1**(1): 52-65.

Morlacchi, S., C. Chiastra, E. Cutrì, P. Zunino, F. Burzotta, L. Formaggia, G. Dubini and F. Migliavacca (2014). "Stent deformation, physical stress, and drug elution obtained with provisional stenting, conventional culotte and Tryton-based culotte to treat bifurcations: A virtual simulation study." EuroIntervention **9**(12): 1441-1453.

Morlacchi, S., B. Keller, P. Arcangeli, M. Balzan, F. Migliavacca, G. Dubini, J. Gunn, N. Arnold, A. Narracott, D. Evans and P. Lawford (2011). "Hemodynamics and In-stent restenosis: Micro-CT images, histology, and computer simulations." Annals of Biomedical Engineering **39**(10): 2615-2626.

Morlacchi, S. and F. Migliavacca (2013). "Modeling stented coronary arteries: Where we are, where to go." Annals of Biomedical Engineering **41**(7): 1428-1444.

Murphy, B. P., P. Savage, P. E. McHugh and D. F. Quinn (2003). "The stress-strain behavior of coronary stent struts is size dependent." Annals of Biomedical Engineering **31**(6): 686-691.

Nakazawa, G. F., A.V.; Vorpahl, M.; Ladich, E.; Kutys, R.; Balazs, I.; Kolodgie, F.D.; Virmani, R. (2009). "Incidence and Predictors of Drug-Eluting Stent Fracture in Human Coronary Artery: A Pathologic Analysis." J Am Coll Cardiol. **54**(21): 1924-1931.

Petrini, L., W. Wu, D. Gastaldi, L. Altomare, S. Farè, F. Migliavacca, A. G. Demir, B. Previtali and M. Vedani (2014). "Development of biodegradable magnesium alloy stents with coating." Frattura ed Integrita Strutturale **8**(29): 364-375.

Pontrelli, G. and F. de Monte (2007). "Mass diffusion through two-layer porous media: an application to the drug-eluting stent." International Journal of Heat and Mass Transfer **50**(17-18): 3658-3669.

Pontrelli, G. and F. De Monte (2009). "Modeling of mass dynamics in arterial drug-eluting stents." Journal of Porous Media **12**(1): 19-28.

Pontrelli, G. and F. de Monte (2010). "A multi-layer porous wall model for coronary drug-eluting stents." International Journal of Heat and Mass Transfer **53**(19-20): 3629-3637.

Rajagopal, K. R., A. R. Srinivasa and A. S. Wineman (2007). "On the shear and bending of a degrading polymer beam." International Journal of Plasticity **23**(9): 1618-1636.

Rogers, C., D. Y. Tseng, J. C. Squire and E. R. Edelman (1999). "Balloon-artery interactions during stent placement: A finite element analysis approach to pressure, compliance, and stent design as contributors to vascular injury." Circulation Research **84**(4): 378-383.

Sakharov, D. V., L. V. Kalachev and D. C. Rijken (2002). "Numerical simulation of local pharmacokinetics of a drug after intravascular delivery with an eluting stent." Journal of Drug Targeting **10**(6): 507-513.

Savage, P., B. P. O'Donnell, P. E. McHugh, B. P. Murphy and D. F. Quinn (2004). "Coronary stent strut size dependent stress-strain response investigated using micromechanical finite element models." Annals of Biomedical Engineering **32**(2): 202-211.

Schwartz, R. S., K. C. Huber, J. G. Murphy, W. D. Edwards, A. R. Camrud, R. E. Vlietstra and D. R. Holmes (1992). "Restenosis and the proportional neointimal response to coronary artery injury: Results in a porcine model." Journal of the American College of Cardiology **19**(2): 267-274.

Shite, J., D. Matsumoto and M. Yokoyama (2006). "Sirolimus-eluting stent fracture with thrombus, visualization by optical coherence tomography." European Heart Journal **27**(12): 1389.

Siepmann, J. and A. Göpferich (2001). "Mathematical modeling of bioerodible, polymeric drug delivery systems." Advanced Drug Delivery Reviews **48**(2-3): 229-247.

Soares, J. S., J. E. Moore and K. R. Rajagopal (2008). "Constitutive framework for biodegradable polymers with applications to biodegradable stents." ASAIO Journal **54**(3): 295-301.

Soares, J. S., J. E. Moore and K. R. Rajagopal (2010). "Modeling of deformation-accelerated breakdown of polylactic acid biodegradable stents." Journal of Medical Devices, Transactions of the ASME **4**(4).

Soares, J. S. and P. Zunino (2010). "A mixture model for water uptake, degradation, erosion and drug release from polydisperse polymeric networks." Biomaterials **31**(11): 3032-3042.

Tahir, H., A. G. Hoekstra, E. Lorenz, P. V. Lawford, D. Rodney Hose, J. Gunn and D. J. W. Evans (2011). "Multi-scale simulations of the dynamics of in-stent restenosis: Impact of stent deployment and design." Interface Focus **1**(3): 365-373.

Tamai, H., K. Igaki, E. Kyo, K. Kosuga, A. Kawashima, S. Matsui, H. Komori, T. Tsuji, S. Motohara and H. Uehata (2000). "Initial and 6-month results of biodegradable poly-l-lactic acid coronary stents in humans." Circulation **102**(4): 399-404.

Tamai, H., K. Igaki, T. Tsuji, E. Kyo, K. Kosuga, A. Kawashima, S. Matsui, H. Komori, S. Motohara, H. Uehata and E. Takeuchi (1999). "A biodegradable poly-l-lactic acid coronary stent in the porcine coronary artery." Journal of Interventional Cardiology **12**(6): 443-449.

Tambača, J. (2003). A Model of Irregular Curved Rods. Applied Mathematics and Scientific Computing. Z. Drmač, V. Hari, L. Sopta, Z. Tutek and K. Veselić, Springer US**:** 289-299.

Tambaca, J., S. Canic, M. Kosor, R. D. Fish and D. Paniagua (2011). "Mechanical behavior of fully expanded commercially available endovascular coronary stents." Texas Heart Institute Journal **38**(5): 491-501.

Tambača, J., M. Kosor, S. Čanic and D. Paniagua (2010). "Mathematical modeling of vascular stents." SIAM Journal on Applied Mathematics **70**(6): 1922-1952.

Tambaĉa, J. and I. Velĉić (2012). "Derivation of the nonlinear bending-torsion model for a junction of elastic rods." Proceedings of the Royal Society of Edinburgh Section A: Mathematics **142**(3): 633-664.

Tambača, J. and B. Žugec (2015). "One-dimensional quasistatic model of biodegradable elastic curved rods." Zeitschrift fur Angewandte Mathematik und Physik.

Tsuji, T., H. Tamai, K. Igaki, E. Kyo, K. Kosuga, T. Hata, M. Okada, T. Nakamura, H. Komori, S. Motohara and H. Uehata (2000). "Experimental and clinical studies of biodegradable polymeric stents." Journal of Interventional Cardiology **13**(6): 439-445.

Tzafriri, A. R., A. Groothuis, G. S. Price and E. R. Edelman (2012). "Stent elution rate determines drug deposition and receptor-mediated effects." Journal of Controlled Release **161**(3): 918-926.

Vergara, C. and P. Zunino (2008). "Multiscale boundary conditions for drug release from cardiovascular stents." Multiscale Modeling and Simulation **7**(2): 565-588.

Weir, N. A., F. J. Buchanan, J. F. Orr and G. R. Dickson (2004). "Degradation of poly-L-lactide. Part 1: In vitro and in vivo physiological temperature degradation." Proceedings of the Institution of Mechanical Engineers, Part H: Journal of Engineering in Medicine **218**(5): 307-319.

Wu, W., S. Chen, D. Gastaldi, L. Petrini, D. Mantovani, K. Yang, L. Tan and F. Migliavacca (2013). "Experimental data confirm numerical modeling of the degradation process of magnesium alloys stents." Acta Biomaterialia **9**(10): 8730-8739.

Wu, W., D. Gastaldi, K. Yang, L. Tan, L. Petrini and F. Migliavacca (2011). "Finite element analyses for design evaluation of biodegradable magnesium alloy stents in arterial vessels."

Materials Science and Engineering B: Solid-State Materials for Advanced Technology **176**(20): 1733-1740.

Wu, W., L. Petrini, D. Gastaldi, T. Villa, M. Vedani, E. Lesma, B. Previtali and F. Migliavacca (2010). "Finite element shape optimization for biodegradable magnesium alloy stents." Annals of Biomedical Engineering **38**(9): 2829-2840.

Zunino, P. (2004). "Multidimensional pharmacokinetic models applied to the design of drug-eluting stents." Cardiovascular Engineering **4**(2): 181-191.

Zunino, P., C. D'Angelo, L. Petrini, C. Vergara, C. Capelli and F. Migliavacca (2009). "Numerical simulation of drug eluting coronary stents: Mechanics, fluid dynamics and drug release." Computer Methods in Applied Mechanics and Engineering **198**(45-46): 3633-3644.

Figures

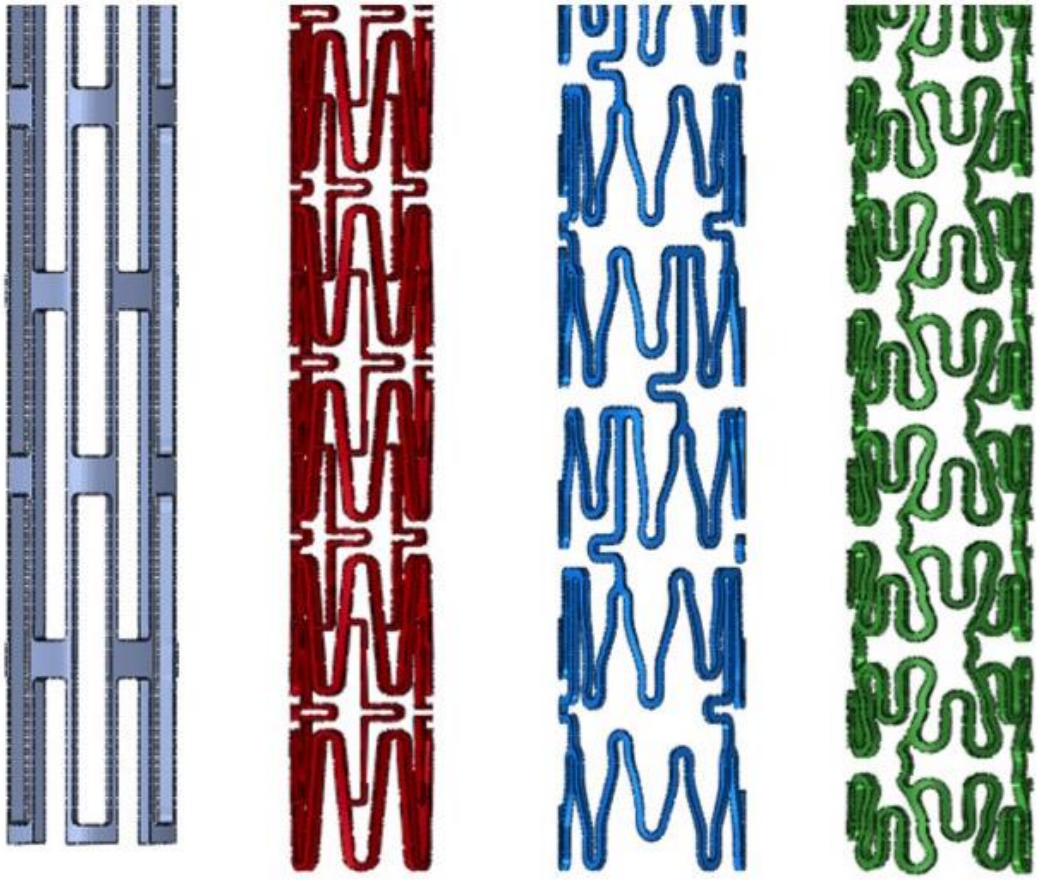

Figure 1: the variety and complexity of patterns in coronary stents. Examples of four CAD models used in computer simulations.

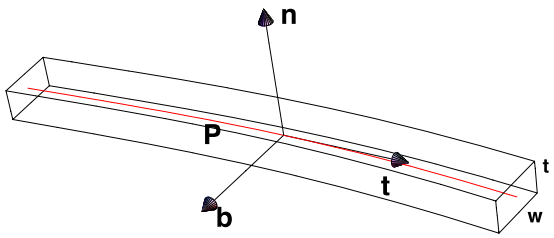

Figure 1. Curved rod with centerline P, and tangent, normal and bi-normal vectors t,n,b.

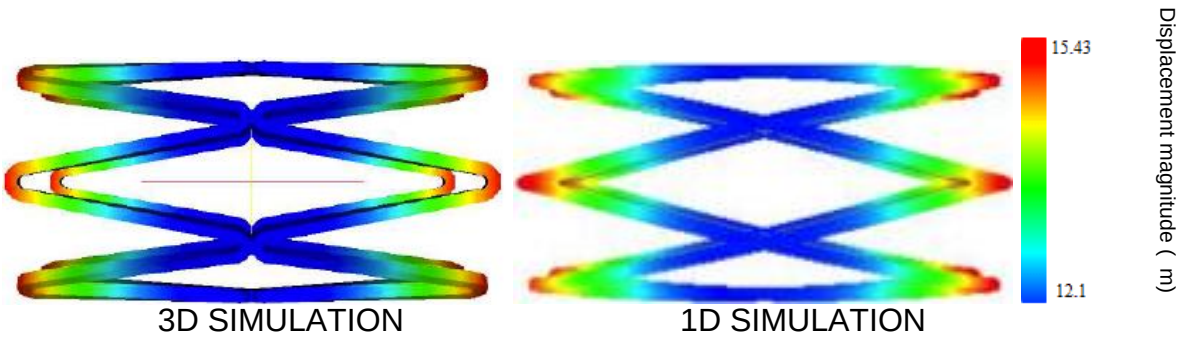

Figure 3 3D (left) and 1D (right) simulation of a uniform stent exposed to a pressure load of 0.5atm. The colors show the magnitude of radial displacement. Pointwise comparison in radial displacement is shown in Fig. 4

.

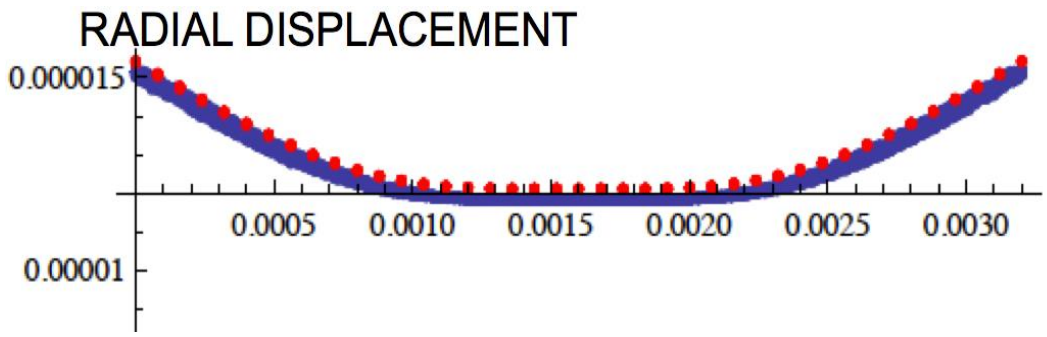

Figure 4: Pointwise comparison in radial displacement between 3D (blue color) and 1D (red dots) simulations. The horizontal axis is stent length.

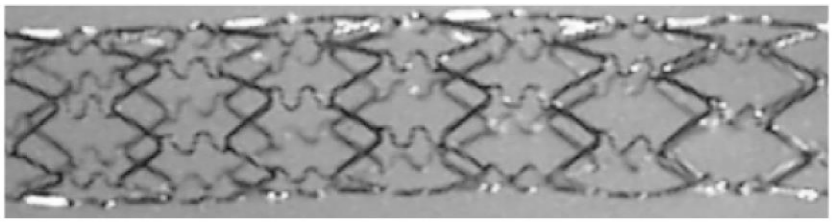

(a) A photograph of Cypher™ stent by Cordis

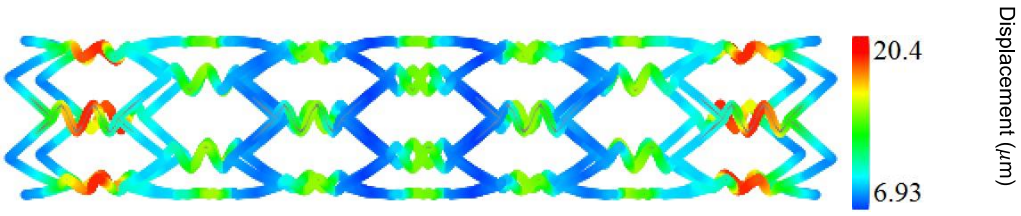

(b) Numerical simulation of Cypher-like stent exposed to uniform pressure of 0.5 atm.

Figure 5: A photo of Cypher stent (top) and numerically generated Cypher-like stent (bottom). The colors on the bottom figure show the displacement magnitude, red denoting large, green denoting intermediate, and blue denoting small displacement after a stent had been exposed to a uniform pressure load of 0.5 atm.

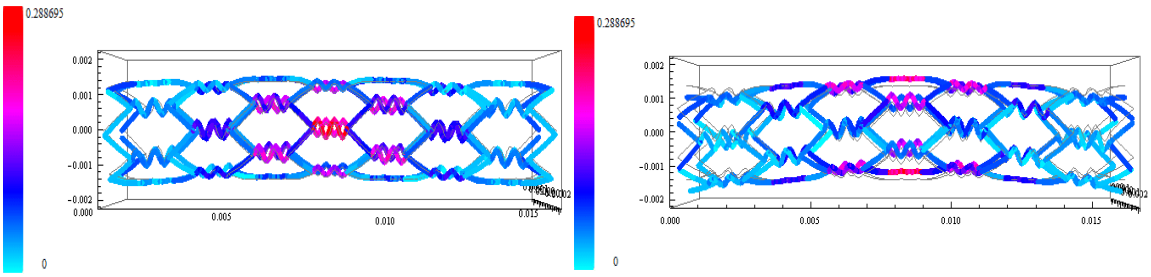

Figure 6: Force magnitude (N) for bent Cypher-like stent model. Left panel shows side view, right panel shows top view. Large force magnitude is observed at sinusoidal struts near the center of the slightly bent stent.

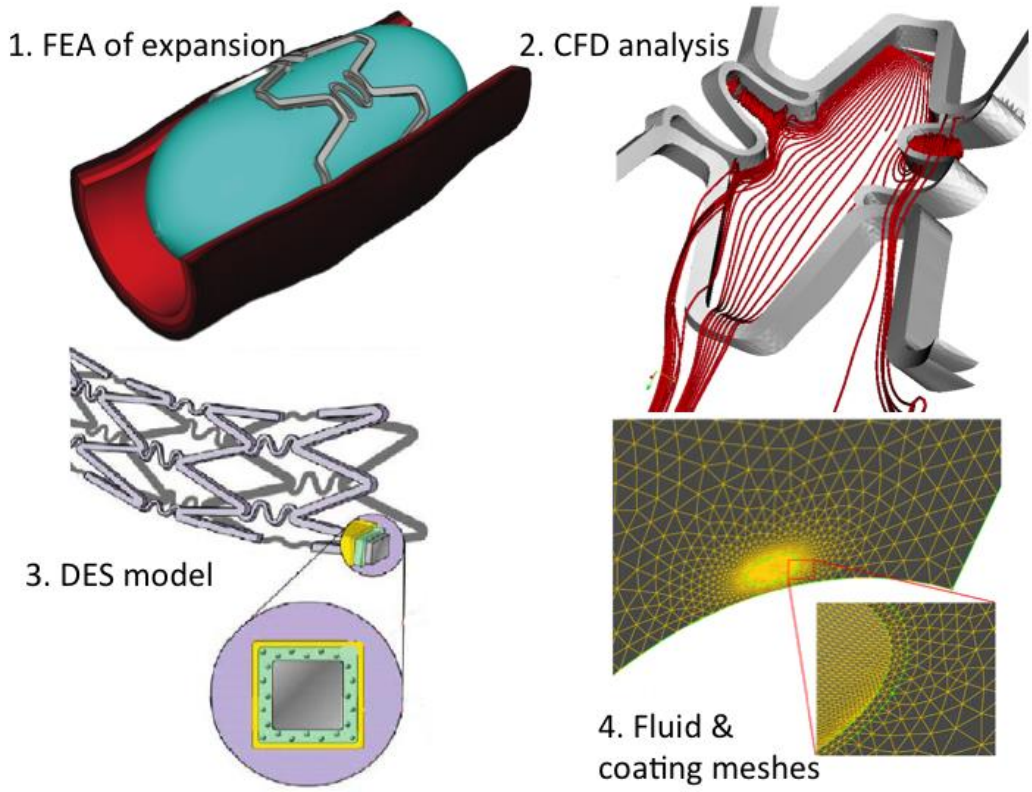

Figure 7: different components needed modeling all aspects of DES (Zunino, D'Angelo et al. 2009)

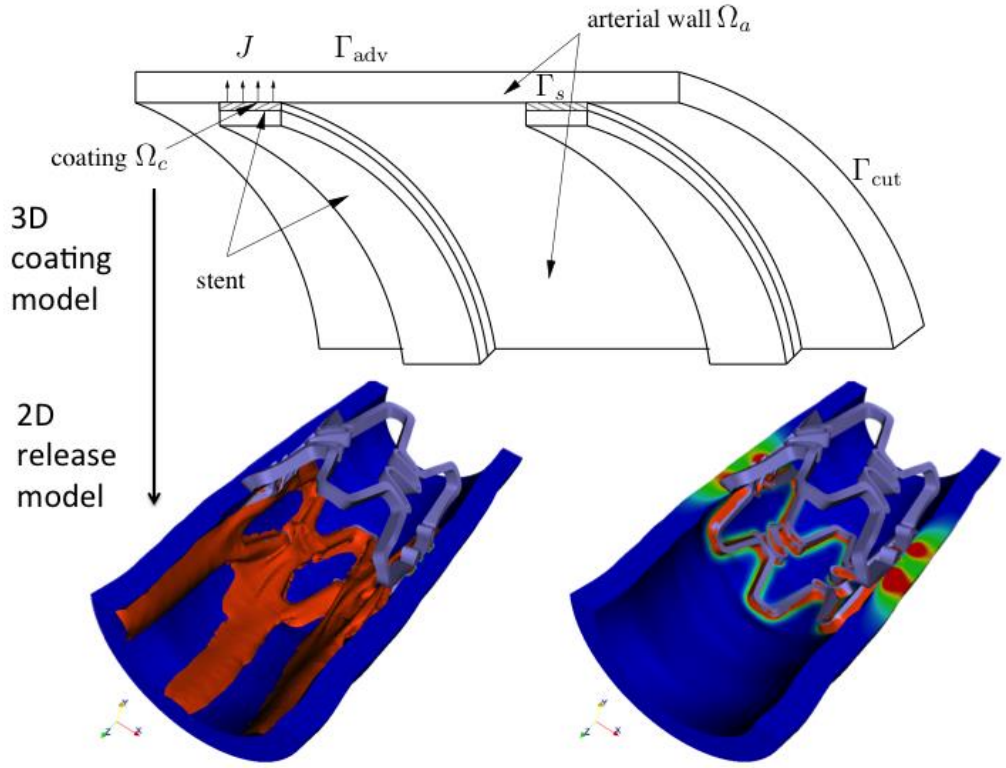

Figure 8: application of Equations 6,7,8 to the simulation of drug release, adapted from (Zunino, D'Angelo et al. 2009)

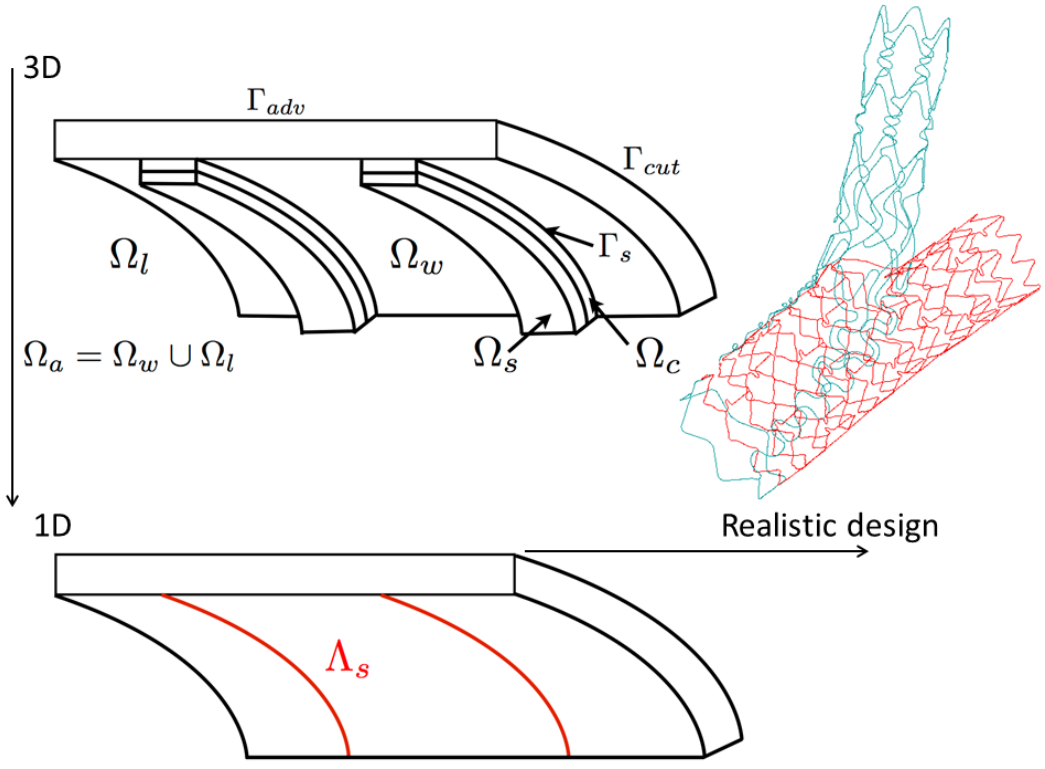

Figure 9: a sketch of the dimensionally reduced model for stent struts

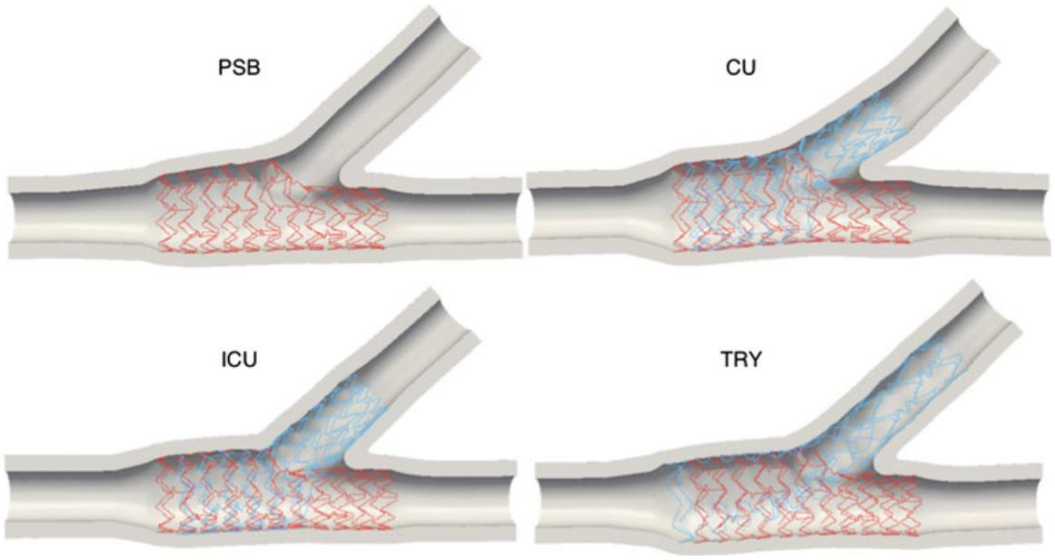

Figure 10: reduced strut model applied for stenting bifurcations with different stenting techniques: Provisional Side Branch (PSB), Culotte, (CU), inverted Culotte (ICU), and the implantation of a newly designed dedicated stent for bifurcations (TRY). Results are from (Cutrì, Zunino et al. 2013)

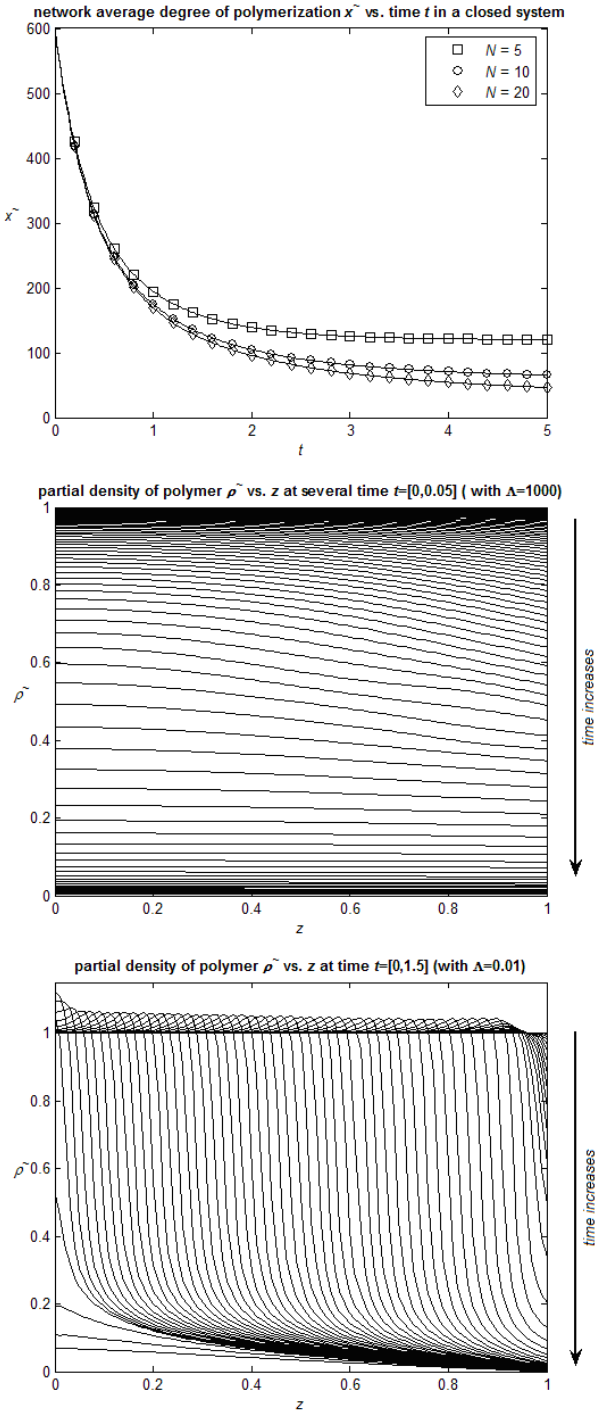

Figure 11: (top panel) Decrease in network average degree of polymerization vs. time in a closed system, where diffusion of species is neglected. (middle panel) Profiles of average polymer density in the diffusion dominated regime. (bottom panel) Profiles of polymer density in the reaction dominated regime.

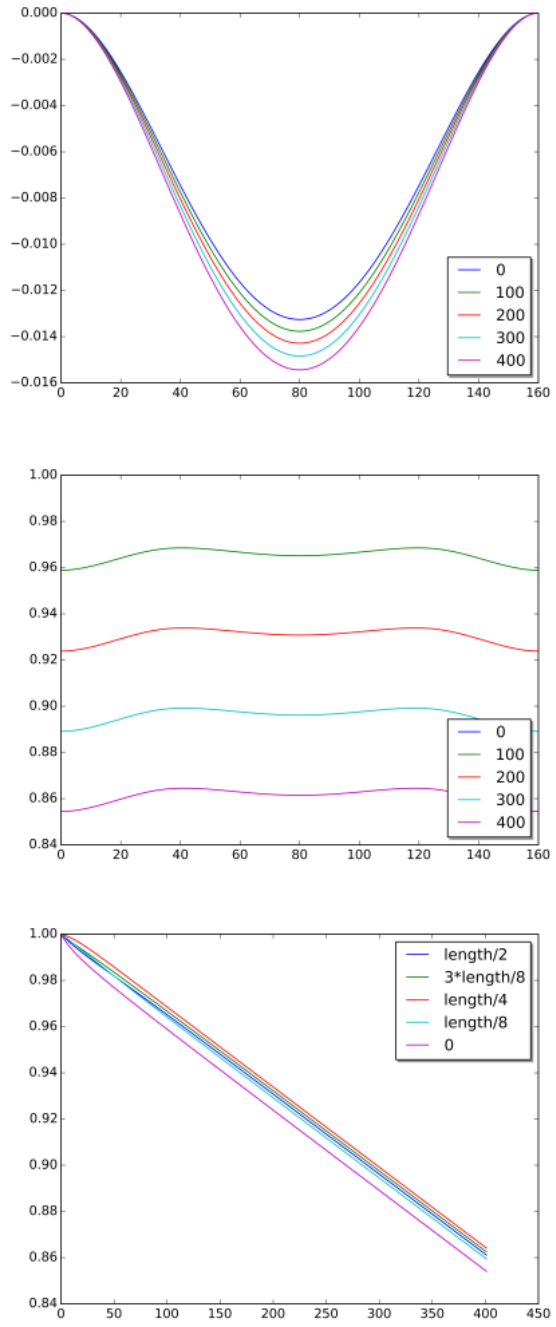

Figure 12: Displacement vs. stent length (top panel), degradation vs. stent length (middle panel) and rate of degradation rate vs. time for a rod clamped at both ends, loaded with a constant contact force (bottom panel). In this case, 400 times steps were calculated.

Click here to download Form for Disclosure of Potential Conflicts of Interest: coi_disclosure.pdf